Progress In Electromagnetics Research M, Vol. 66, 109–118, 2018

Symplectic Pseudospectral Time-Domain Scheme for Solving Time-Dependent Schrödinger Equation

Jing Shen*[,1], Wei E. I. Sha[3], Xiaojing Kuang[1], Jinhua Hu[1], Zhixiang Huang[2], and Xianliang Wu[2]

Abstract—A symplectic pseudospectral time-domain (SPSTD) scheme is developed to solve Schrödinger equation. Instead of spatial finite differences in conventional finite-difference time-domain (FDTD) methods, fast Fourier transform is used to calculate spatial derivatives. In time domain, the scheme adopts high-order symplectic integrators to simulate time evolution of Schrödinger equation. A detailed numerical study on the eigenvalue problems of 1D quantum well and 3D harmonic oscillator is carried out. The simulation results strongly confirm the advantages of the SPSTD scheme over the traditional PSTD method and FDTD approach. Furthermore, by comparing to the traditional PSTD method and the non-symplectic Runge-Kutta (RK) method, the explicit SPSTD scheme, which is an infinite order of accuracy in space domain and energy-conserving in time domain, is well suited for a long-term simulation.

1. INTRODUCTION

Numerical solution to Schrödinger equation has become increasingly important because of the tremendous demands for the design and optimization of nanodevices, where quantum effects are significant or dominant [1]. The eigenvalue problem of Schrödinger equation is fundamentally important for quantum transport and nanodevice modeling. One of commonly adopted methods to solve the eigenvalue problem of Schrödinger equation is FDTD method [2, 3]. In FDTD method, spatial derivatives in Schrödinger equation are approximated by finite differences. The Yee algorithm has a second-order accuracy both in space and time. Thus, a fine discretization is required to obtain a desired result tailored to physical designs. To reduce the complexity of time-domain solutions by decreasing grid density, we employ an efficient and accurate approach called pseudospectral method. The pseudospectral method has an infinite order of accuracy since Fourier transform is utilized to represent the spatial derivatives [4, 5]. Numerical experiments have shown that the pseudospectral time-domain (PSTD) method is a factor of $4^D - 8^D$ more efficient than the FDTD method (where D is the dimension number [6–9]).

Many important physical phenomena can be modeled by Hamiltonian differential equations [10–12]. The time evolution of Hamiltonian is essentially a symplectic transform. Equivalently, Hamiltonian flow conserves the symplectic structure [10–16]. The symplectic schemes are the time-steeping strategies designed to preserve the global symplectic structure of the phase space of a Hamiltonian system. Symplectic schemes have proven themselves to be one of best candidates for numerically modeling the Hamiltonian system, especially for a long-term simulation. The symplectic scheme has been applied to solve Schrödinger equation, and numerical examples have been shown [17, 18]. In this paper, we

Received 8 January 2018, Accepted 17 March 2018, Scheduled 27 March 2018

* Corresponding author: Jing Shen (jingsh@hfnu.edu.cn).

[1] School of Electronics and Information Engineering, Hefei Normal University, Hefei, Anhui, China. [2] School of Electronics and Information Engineering, Anhui University, Hefei, Anhui, China. [3] School of Electronics and Information Engineering, Zhejiang University, Hangzhou, Zhejiang, China.

integrate the pseudospectral method with symplectic schemes to construct a symplectic pseudospectral time-domain (SPSTD) scheme for solving Schrödinger equations.

2. THEORY

2.1. Construction of the Algorithm

The time-dependent Schrödinger equation is given by [2]

$$i\hbar\frac{\partial\psi(\mathbf{r},t)}{\partial t}=-\frac{\hbar^2}{2m^*}\nabla^2\psi(\mathbf{r},t)+V(\mathbf{r})\psi(\mathbf{r},t) \tag{1}$$

where $\psi(\mathbf{r},t)$ is the wave function that is a probability amplitude describing the quantum state of a particle at the position $\mathbf{r}$ and time t; m^* is the (effective) mass of the particle; $-\frac{\hbar^2}{2m^*}\nabla^2$ is the kinetic energy operator; $V(\mathbf{r})$ is the time-independent potential energy; $-\frac{\hbar^2}{2m^*}\nabla^2+V$ is the Hamiltonian operator. To avoid using complex numbers, one can separate the variable $\psi(\mathbf{r},t)$ into its real and imaginary parts as

$$\psi(\mathbf{r},t)=\psi_R(\mathbf{r},t)+i\psi_I(\mathbf{r},t). \tag{2}$$

Inserting Eq. (2) into Eq. (1), we can get the following coupled set of equations [3]

$$\hbar\frac{\partial\psi_R(\mathbf{r},t)}{\partial t}=-\frac{\hbar^2}{2m^*}\left[\begin{array}{l}\dfrac{\partial^2\psi_I(\mathbf{r},t)}{\partial x^2}\\ +\dfrac{\partial^2\psi_I(\mathbf{r},t)}{\partial y^2}\\ +\dfrac{\partial^2\psi_I(\mathbf{r},t)}{\partial z^2}\end{array}\right]+V(\mathbf{r})\psi_I(\mathbf{r},t), \tag{3}$$

$$\hbar\frac{\partial\psi_I(\mathbf{r},t)}{\partial t}=\frac{\hbar^2}{2m^*}\left[\begin{array}{l}\dfrac{\partial^2\psi_R(\mathbf{r},t)}{\partial x^2}\\ +\dfrac{\partial^2\psi_R(\mathbf{r},t)}{\partial y^2}\\ +\dfrac{\partial^2\psi_R(\mathbf{r},t)}{\partial z^2}\end{array}\right]-V(\mathbf{r})\psi_R(\mathbf{r},t). \tag{4}$$

A mesh is defined in a discrete set of grid points that sample the wave function in space and time. The real and imaginary parts of the wave function can be represented as

$$\psi_R(\mathbf{r},t)\approx\psi_R^n(i,j,k)=\psi_R(i\Delta_x,j\Delta_y,k\Delta_z,n\Delta_t), \tag{5}$$

$$\psi_I(\mathbf{r},t)\approx\psi_I^n(i,j,k)=\psi_I(i\Delta_x,j\Delta_y,k\Delta_z,n\Delta_t), \tag{6}$$

where Δ_x, Δ_y , and Δ_z are, respectively, the spatial steps in the x, y, and z coordinate directions; Δ_t is the time step; i, j, k and n are integers.

Regarding the pseudospectral method in space, we take the Fourier series expansion

$$f(x)=\sum_{n=-\infty}^{+\infty}a_n e^{iK_n x}, \tag{7}$$

with

$$a_n=\frac{1}{L}\int_0^L f(x)e^{-iK_n x}\mathrm{d}x=F_x[f(x)], \tag{8}$$

where L is the periodicity of the structure; $K_n=2\pi n/L$; $n=0,\pm1,\pm2,\cdots$; F_x stands for the forward Fourier transforms in the x direction. The corresponding spatial derivatives can be obtained by

$$\frac{\mathrm{d}f}{\mathrm{d}x}=\sum_{n=-\infty}^{+\infty}iK_n a_n e^{iK_n x}=F_x^{-1}\{iK_n F_x[f(x)]\}, \tag{9}$$

where F_x^{-1} stands for the inverse Fourier transforms in the x direction. The forward and inverse Fourier transforms can be fast and efficiently computed by fast Fourier transform (FFT) algorithms. For second-order derivatives, we have

$$\frac{\partial^2 \psi_I}{\partial x^2} = F_x^{-1}\left\{iK_n F_x\left[F_x^{-1}\left\{iK_n F_x\left[\psi_I\left(\mathbf{r},t\right)\right]\right\}\right]\right\}. \tag{10}$$

It should be noted that only real parts of results remain after each inverse Fourier transform. Therefore, with the help of Fourier transforms, Eqs. (3) and (4) can be rewritten as

$$\begin{aligned}
&\psi_R^{n+1}(i,j,k) = \psi_R^n(i,j,k) \\
&-\frac{\hbar\Delta t}{2m^*}\left[F_x^{-1}\left(iK_x F_x\left(F_x^{-1}\left(iK_x F_x\left(\psi_I^n(i,j,k)\right)\right)\right)\right)\right] \\
&-\frac{\hbar\Delta t}{2m^*}\left[F_y^{-1}\left(iK_y F_y\left(F_y^{-1}\left(iK_y F_y\left(\psi_I^n(i,j,k)\right)\right)\right)\right)\right] \\
&-\frac{\hbar\Delta t}{2m^*}\left[F_z^{-1}\left(iK_z F_z\left(F_z^{-1}\left(iK_z F_z\left(\psi_I^n(i,j,k)\right)\right)\right)\right)\right] \\
&+\frac{V(i,j,k)\,\Delta t}{\hbar} \times \psi_I^{n+1/2}(i,j,k)
\end{aligned} \tag{11}$$

$$\begin{aligned}
&\psi_I^{n+1}(i,j,k) = \psi_I^n(i,j,k) \\
&+\frac{\hbar\Delta t}{2m^*}\left[F_x^{-1}\left(iK_x F_x\left(F_x^{-1}\left(iK_x F_x\left(\psi_R^n(i,j,k)\right)\right)\right)\right)\right] \\
&+\frac{\hbar\Delta t}{2m^*}\left[F_y^{-1}\left(iK_y F_y\left(F_y^{-1}\left(iK_y F_y\left(\psi_R^n(i,j,k)\right)\right)\right)\right)\right] \\
&+\frac{\hbar\Delta t}{2m^*}\left[F_z^{-1}\left(iK_z F_z\left(F_z^{-1}\left(iK_z F_z\left(\psi_R^n(i,j,k)\right)\right)\right)\right)\right] \\
&-\frac{V(i,j,k)\,\Delta t}{\hbar} \times \psi_R^{n+1/2}(i,j,k)
\end{aligned} \tag{12}$$

In order to implement the symplectic algorithm, we notate a wave function of space and time at a discrete stage in the time step as

$$\psi(i,j,k) = \psi^{n+l/m}(i\Delta_x, j\Delta_y, k\Delta_z, (n+\tau_l)\Delta_t) \tag{13}$$

where $n+l/m$ denotes the lth stage after n time steps, m the total stage number, and τ_l the fixed time with respect to the lth stage. With the help of Eqs. (3) and (4), the Schrödinger equation can be casted into a matrix form

$$\frac{\partial}{\partial t}\begin{pmatrix}\psi_R\\ \psi_I\end{pmatrix} = L\begin{pmatrix}\psi_R\\ \psi_I\end{pmatrix} = (A+B)\begin{pmatrix}\psi_R\\ \psi_I\end{pmatrix} \tag{14}$$

$$A = \begin{pmatrix}0 & K\\ 0 & 0\end{pmatrix}, B = \begin{pmatrix}0 & 0\\ -K & 0\end{pmatrix} \tag{15}$$

$$K = -\frac{\hbar}{2m^*}\left(\frac{\partial}{\partial x^2} + \frac{\partial}{\partial y^2} + \frac{\partial}{\partial z^2}\right) + \frac{V}{\hbar}, \tag{16}$$

where $A^v = 0$ and $B^v = 0$ if $v \geq 2$. It is easy to prove that L in Eq. (14) is an asymmetric operator. and therefore. the exact solution of Schrödinger equation $\exp(Lt)$ is an orthogonal operator conserving the total energy of quantum system. Using the product of elementary symplectic mapping, the exact solution of Eq. (14) from $t = 0$ to $t = \Delta_t$ can be approximately

$$\exp(\Delta_t(A+B)) = \prod_{l=1}^{m}\exp(d_l\Delta_t B)\exp(c_l\Delta_t A) + O({\Delta_t}^{p+1}) = \prod_{l=1}^{m}(1+d_l\Delta_t B)(1+c_l\Delta_t A) + O({\Delta_t}^{p+1}) \tag{17}$$

where c_l and d_l are the coefficients of symplectic integrators, and p is the order of the approximation. The symplectic integrators can satisfy the time-reversible or symmetric condition [19, 20]. The detailed update equation for the real part of the wave function at the lth stage can be written as

$$\begin{aligned}
&\psi_R^{n+l/m}(i,j,k) = \psi_R^{n+(l-1)/m}(i,j,k) \\
&-\alpha\left[F_x^{-1}\left(iK_xF_x\left(F_x^{-1}\left(iK_xF_x\left(\psi_I^{n+l/m}(i,j,k)\right)\right)\right)\right)\right] \\
&-\alpha\left[F_y^{-1}\left(iK_yF_y\left(F_y^{-1}\left(iK_yF_y\left(\psi_I^{n+l/m}(i,j,k)\right)\right)\right)\right)\right] \\
&-\alpha\left[F_z^{-1}\left(iK_zF_z\left(F_z^{-1}\left(iK_zF_z\left(\psi_I^{n+l/m}(i,j,k)\right)\right)\right)\right)\right] \\
&+\frac{V(i,j,k)\,c_l\Delta t}{\hbar}\times\psi_I^{n+l/m}(i,j,k),
\end{aligned} \tag{18}$$

where $\alpha = \frac{\hbar c_l \Delta_t}{2m^*}$. Here the fourth-order symmetric symplectic integrators are employed, i.e. $c_1 = 0.26833010$, $c_2 = -0.18799162$, $c_3 = 0.91966152$, and $d_l = c_{m-l+1}$ $(1 \le l \le m)$.

2.2. Stability Analysis of SPSTD Algorithm and Boundary Conditions

According to the von Neumann stability method, the solution of the wave function can be represented as a superposition of plane-waves

$$\psi(x,y,z,t) = A_0 \exp\left(-j_0(k_x x + k_y y + k_z z)\right) \tag{19}$$

where $k_x = k_0 \sin\theta\cos\varphi, k_y = k_0 \sin\theta\sin\varphi, k_z = k_0\cos\theta, k_0 = \frac{p_m}{\hbar}$ is the wave number, p_m the momentum, and θ and φ are the spherical angles. The qth-order collocated differences are used to discretize the second-order spatial derivatives, i.e.

$$\frac{\partial^2\psi}{\partial z^2} = \frac{\partial^2 A_0 \exp\left(-j_0\left(k_x x + k_y y + k_z z\right)\right)}{\partial z^2} = -k_z^2\psi, \tag{20}$$

For simplicity, we consider a 1D Schrödinger equation with zero potential energy

$$\frac{\partial}{\partial t}\begin{pmatrix}\psi_R\\ \psi_I\end{pmatrix} = \begin{pmatrix} 0 & -\frac{\hbar}{2m^*}\frac{\partial^2}{\partial z^2} \\ \frac{\hbar}{2m^*}\frac{\partial^2}{\partial z^2} & 0\end{pmatrix}\begin{pmatrix}\psi_R\\ \psi_I\end{pmatrix}, \tag{21}$$

and corresponding spatial discretization form is given by

$$\frac{\partial}{\partial t}\begin{pmatrix}\psi_R\\ \psi_I\end{pmatrix} = \begin{pmatrix} 0 & \frac{\hbar}{2m^*}k_z \\ -\frac{\hbar}{2m^*}k_z & 0\end{pmatrix}\begin{pmatrix}\psi_R\\ \psi_I\end{pmatrix}, \tag{22}$$

It is trivial to access the discretized evolution matrix L^d with the high-order symplectic integration scheme

$$L^d = \begin{bmatrix} l_{11} & l_{12} \\ l_{21} & l_{22}\end{bmatrix} = \prod_{l=1}^{m}\begin{pmatrix} 1 & 0 \\ -\frac{\hbar}{2m^*}k_z d_l \Delta_t & 1\end{pmatrix}\begin{pmatrix} 1 & \frac{\hbar}{2m^*}k_z c_l \Delta_t \\ 0 & 1\end{pmatrix}, \tag{23}$$

The eigenvalues λ of the evolution matrix satisfy the following eigen-equation

$$\lambda^2 - tr(L^d)\lambda + \det(L^d) = 0, \tag{24}$$

where $tr(L^d)$ and $\det(L^d)$ are the trace and determinant of the evolution matrix, respectively. The discretized evolution matrix is a symplectic matrix with the determinant of 1. The eigen-equation then can be simplified as

$$\lambda^2 - tr(L^d)\lambda + 1 = 0, \tag{25}$$

and its solutions are $\lambda_{1,2} = \frac{tr(L^d) \pm j_0\sqrt{4-\left[tr(L^d)\right]^2}}{2}$. A stable algorithm requires $|\lambda_{1,2}| = 1$, and thus $|tr(L^d)| \leq 2$. Implementing terms of matrix multiplications, we can get

$$tr(L^d) = 2 + \sum_{l=1}^{m} (-1)^l g_l \left(\left(\frac{\hbar}{2m^*} \right)^2 \Delta_t^2 k_z^2 \right)^l \tag{26}$$

$$tr(L^d) = 2 + \sum_{l=1}^{m} (-1)^l g_l \left(\left(\frac{\hbar}{2m^*} \right)^2 \Delta_t^2 k_z^2 \right)^l \tag{27}$$

$$g_l = \sum_{1 \leq i_1 \leq j_1 < i_2 \leq j_2 < \cdots < i_l \leq j_l \leq m} c_{i_1} d_{j_1} c_{i_2} d_{j_2} \cdots c_{i_l} d_{j_l} + \sum_{1 \leq i_1 < j_1 \leq i_2 < j_2 \leq \cdots \leq i_l < j_l \leq m} d_{i_1} c_{j_1} d_{i_2} c_{j_2} \cdots d_{i_l} c_{j_l} \tag{28}$$

The above results can be generalized to a 3D Schrödinger equation with zero potential energy, i.e.

$$tr(L^d) = 2 + \sum_{l=1}^{m} (-1)^l g_l \left(\left(\frac{\hbar}{2m^*} \right)^2 \Delta_t^2 (k_x + k_y + k_z)^2 \right)^l \tag{29}$$

Finally we can get

$$\sqrt{\frac{\hbar}{m^*} \frac{\Delta_t}{{\Delta_\delta}^2}} \leq CFL, \tag{30}$$

where CFL is the Courant-Friedrichs-Levy (CFL) number. Table 1 lists the maximum stability (CFL number) of the traditional FDTD method, PSTD approach, and SPSTD scheme. The symmetric symplectic integrators for the SPSTD scheme are given as follows: $c_1 = 0.26833010$, $c_2 = -0.18799162$, $c_3 = 0.91966152$, and $d_l = c_{m-l+1} (1 \leq l \leq m)$. From the table, the stability of the SPSTD scheme [6] is larger than that of the traditional PSTD method through a careful optimization of symplectic integrators.

Table 1. The numerical stability for various algorithms. $D = 1, 2, 3$ is the dimension number.

Algorithm	CFL Number
FDTD	$\frac{1}{\sqrt{D}}$
PSTD	$\frac{2}{\sqrt{D\pi}}$
SPSTD	$1.503 \times \frac{2}{\sqrt{D\pi}}$

To guarantee the numerical accuracy of simulation, boundary conditions should be handled properly. Regarding periodic boundary condition or fast decayed wave function, we employ discrete Fourier transform (DFT) to represent the spatial derivatives as shown in Eqs. (9). Regarding the Dirichlet boundary condition (for modeling the infinite potential well), discrete Sine Transform (DST) should be chosen to replace the DFT. Regarding the Neumann boundary condition, discrete Cosine transform (DCT) should be adopted.

3. NUMERICAL RESULTS

3.1. 1D Schrödinger Equation

For the first example, we consider a particle in a one-dimensional (1D) infinite potential well. The simulation domain and cell size depend on the length of the box to be simulated and the highest eigenenergy of the particle of interest, respectively. Without the loss of generality, we choose the domain to be L=1 nm, the cell size $\Delta x = 0.1$ nm, the time step $\Delta t = (m^*/4\hbar)(\Delta x)^2 = 0.0216$ fs and the iteration step $N_{\max} = 1024$. The eigenenergies of the quantum well are quantized as,

$$E_n = \frac{\hbar^2 \pi^2}{2m^* a^2} n^2, n = 1, 2, 3, \ldots \tag{31}$$

Table 2. The eigenfrequency comparisons for a 1D quantum well.

Algorithm	FDTD	PSTD	SPSTD	Analytical
ω_1	0.5683	0.5683	0.5683	0.5713
ω_2	2.2731	2.2731	2.2731	2.2852
ω_3	4.8303	5.1145	5.1145	5.1416
ω_4	7.9558	9.0924	9.0924	9.1406
ω_5	11.6496	14.4910	14.2068	14.2823
ω_6	15.3434	20.7420	20.4578	20.5665
ω_7	18.4689	28.1295	27.8454	27.9932
ω_8	22.7309	37.5060	36.6536	36.5626

In order to excite all possible modes, the delta source is located at the center of the box with two grids offset. Table 2 lists the calculated eigenfrequencies. Compared with the analytical solutions, SPSTD scheme can achieve the best accuracy. Using $\Delta x = 0.05\,\text{nm}$, Fig. 1 and Fig. 2 show the eigenstates corresponding to the eigenfrequencies ω_4 and ω_5, respectively. Both the SPSTD and PSTD schemes can achieve much better results than the FDTD method.

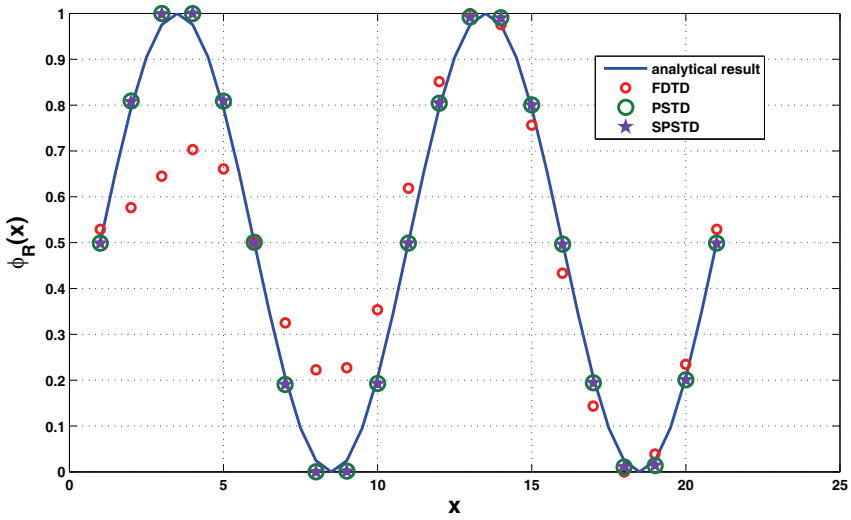

Figure 1. The normalized eigenstate (the real part of the wave function) corresponding to the eigenfrequency ω_4 for a 1D quantum well.

The normalized condition of the wave function should be conserved under a long-term simulation, which determines energy-conserving property of Schrödinger equation. In order to testify the property, we proceed to solve the 1D quantum well numerically using the SPSTD method, PSTD method and a non-symplectic Runge-Kutta (RK) method. In order to testify the energy-conserving property, the time evolution of the system is executed from $t = 0$ to $t = 3300$ using different time steps of $\Delta t = 0.2\Delta t_q$ and $\Delta t = \Delta t_q$ ($\Delta t_q = 0.0013\,\text{fs}$, $L = 1\,\text{nm}$, and $\Delta x = 0.025\,\text{nm}$). Fig. 3 shows the integrated wave function $\int |\psi(x)|^2\,dx$ over the quantum well region by using various approaches. The SPSTD scheme holds the normalized condition of the wave function better.

3.2. 2D Schrödinger equation

The simulation domain is set to $L_x \times L_y = 1\,\text{nm} \times 1\,\text{nm}$, $\Delta x = \Delta y = 0.1\,\text{nm}$, the time step $\Delta t = (m^*/8\hbar)\,(\Delta x)^2 = 0.0108\,\text{fs}$ and the iteration step $N_{\max} = 2048$. Table 3 lists the calculated

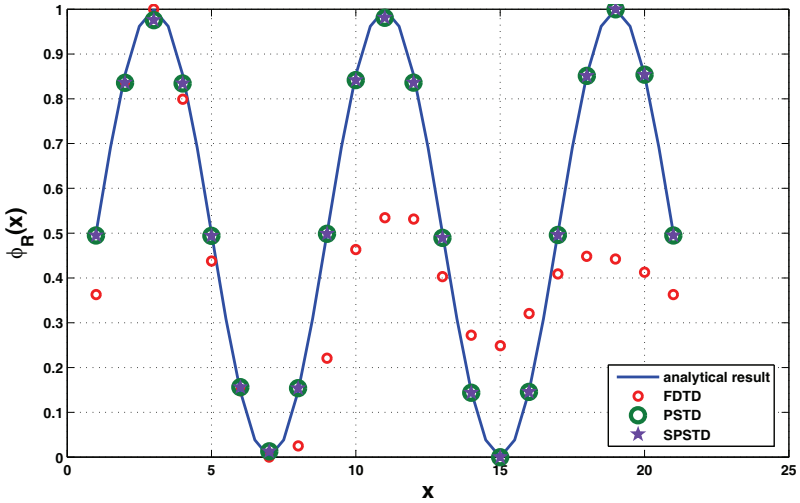

Figure 2. The normalized eigenstate (the real part of the wave function) corresponding to the eigenfrequency ω_5 for a 1D quantum well.

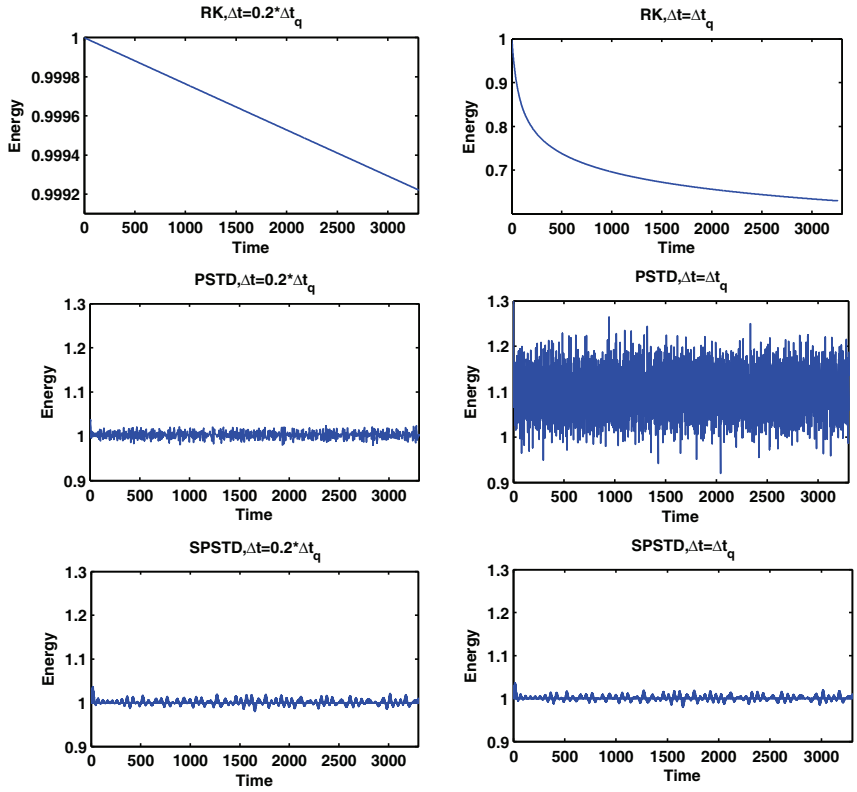

Figure 3. The time evolution of the integrated wave function $\int |\psi(x)|^2 \, dx$ over a 1D quantum well region.

eigenfrequencies, and Fig. 1 show the eigenstates corresponding to the eigenfrequencies ω_{22}. Compared with the analytical solution. The SPSTD scheme achieves best accuracy.

3.3. 3D Schrödinger equation

We consider a three-dimensional (3D) isotropic quantum harmonic oscillator, where the potential energy $V(x, y, z) = \frac{1}{2}k(x^2 + y^2 + z^2)$. The simulation domain is set to $L_x \times L_y \times L_z = 1\,\text{nm} \times 1\,\text{nm} \times 1\,\text{nm}$,

Table 3. The eigenfrequency comparisons for a 2D quantum well.

Algorithm	FDTD	PSTD	SPSTD	Analytical
ω_{11}	1.1366	1.1366	1.1366	1.1426
ω_{12}	2.6283	2.8413	2.8413	2.8565
ω_{22}	4.1909	4.4039	4.5459	4.5703
ω_{13}	5.1855	5.8245	5.6825	5.7129
ω_{23}	6.3221	7.6718	7.4588	7.4268
ω_{14}	8.0978	10.0160	9.7314	9.7119
ω_{44}	14.9169	18.6818	18.2558	18.2813

Table 4. The eigenfrequency comparisons for a 3D quantum harmonic oscillator.

Algorithm	FDTD	PSTD	SPSTD	Analytical
ω_{000}	9.6606	9.9448	9.9448	9.9896
ω_{001}	15.9116	16.7641	16.7641	16.6493
ω_{011}	22.1626	23.2992	23.2992	23.3090
ω_{111}	28.1295	30.1185	29.8343	29.9687
ω_{112}	35.5171	36.9377	36.6536	36.6284
ω_{122}	42.0521	43.7570	43.4729	43.2881
ω_{222}	49.1556	51.7128	50.2922	49.9479
ω_{223}	52.5653	58.8163	57.1114	56.6076

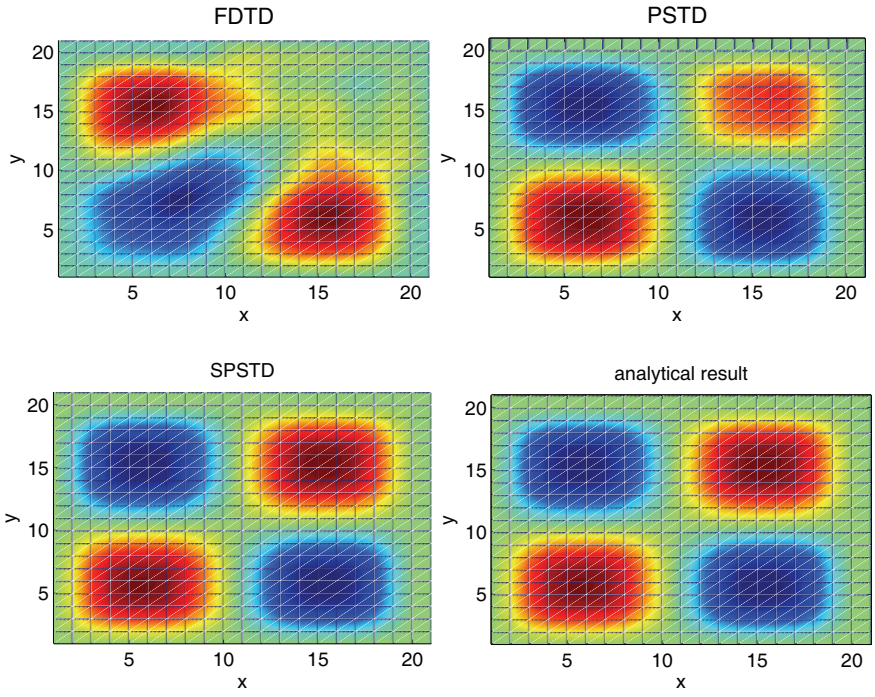

Figure 4. The normalized eigenstate (the real part of the wave function) corresponding to the eigenfrequency ω_{22} for a 2D quantum well.

$\Delta x = \Delta y = \Delta z = 0.1\,\text{nm}$, the time step $\Delta t = (m^*/8\hbar)(\Delta x)^2 = 0.0108\,\text{fs}$ and the iteration step $N_{\max} = 2048$. The eigenenergies of the harmonic oscillator are

$$E_{n_x,n_y,n_z} = (n_x + n_y + n_z + 1.5)\,\hbar\omega \tag{32}$$

Table 4 lists the calculated eigenfrequencies. Compared with the analytical solution, the SPSTD scheme achieves the best accuracy.

4. CONCLUSION

We have developed an SPSTD for solving time-dependent Schrödinger equation. On one hand, the scheme has an infinite-order accuracy by using Fourier transforms to represent the spatial derivatives. On the other hand, incorporating the symplectic integrators in the time domain, the scheme demonstrates excellent numerical performances under a long-term simulation. Our numerical results validate significant advantages of the SPSTD scheme in solving the eigenvalue problem of Schrödinger equation. The work is fundamentally important for the quantum device simulation.

ACKNOWLEDGMENT

This work was supported by the National Natural Science Foundation of China (61301062, 51207041, 61471001,61601166,61701163), the Key Project of Provincial Natural Science Research of University of Anhui Province of China (KJ2015A260).

REFERENCES

1. Datta, S., *Quantum Transport: Atom to Transistor*, Cambridge University Press, New York, 2005.
2. Soriano, A., A. E. Navarro, A. J. Porti, and V. Such, "Analysis of the finite difference time domain technique to solve the Schrodinger equation for quantum devices," *J. Appl. Phys.*, Vol. 95, No. 12, 8011–8018, 2004.
3. Sullivan, D. M. and D. S. Citrin, "Determining quantum eigenfunctions in three dimensional nanoscale structures," *J. Appl. Phys.*, Vol. 97, No. 10, 581–592, 2005.
4. Cai, J. X. and Y. S. Wang, "A conservative Fourier pseudospectral algorithm for a coupled nonlinear Schrödinger system," *Chin. Phys. B*, Vol. 22, No. 6, 135–140, 2013.
5. He, J. P., L. F. Shen, Q. Zhang, and S. L. He, "A pseudospectral time-domain algorithm for calculating the band structure of a two-dimensional photonic crystal," *Chin. Phys. Lett.*, Vol. 19, No. 4, 507–510, 2002.
6. Liu, Q. H., "The PSTD algorithm: A time-domain method requiring only two cells per wavelength," *Microw. Opt. Technol. Lett.*, Vol. 15, 158–165, 1997.
7. Brendan, B. G., "Improved numerical cherenkov instability suppression in the generalized PSTD PIC algorithm," *Computer Physics Communications*, Vol. 196, 221–225, 2015.
8. Mechthild, T. and J. Siam, "Convergenceanalysis of high-order time-spliting pseudospectral methods for nonlinear Schrödinger equation," *SIAM J. Numer. Anal.*, Vol. 50, No. 6, 3231–3258, 2012.
9. Shi, Y. and C. H. Liang, "Analysis of the left-handed metamaterials using multi-domain pseudospectral time-domain algorithm," *Progress In Electromagnetics Research*, Vol. 51, 153–165, 2005.
10. Sanz, J. M. and M. P. Calvo, *Numerical Hamiltonian Problems*, Mathematics of Computation, Vol. 64, No. 5, 21–24, 1994.
11. Sheu, T. W. H., R. Y. Chung, and J. H. Li,"Development of a symplectic scheme with optimized numerical dispersion-relation equation to solve Maxwell's equations in dispersive media," *Progress In Electromagnetics Research*, Vol. 132, 517–549, 2012.
12. Guyenne, P., D. Nicholls, and C. Sulem, *Hamiltonian Partial Differential Equations and Applications*, Springer, New York, 2015.

13. Tao, M., "Explicit symplectic approximation of nonseparable Hamiltonians: Algorithm and long time performance," *Physical Review E.*, Vol. 94, No. 4, 3303, 2016.
14. Sun, Y. and P. S. P. Tse, "Symplectic and multisymplectic numerical methods for Maxwells equations," *J. Comput. Phys.*, Vol. 230, No. 5, 2076–2094, 2011.
15. Monovasilis, T., Z. Kalogiratou, and T. E. Simos, "Families of third and fourth algebraic order trigonometrically fitted symplectic methods for the numerical integration of Hamiltonian systems," *Comput. Phys. Commun.*, Vol. 177, No. 10, 757–763, 2007.
16. Chen, Z. X., X. You, and W. Shi, "Symmetric and symplectic ERKN methods for oscillatory Hamiltonian systems," *Comput. Phys. Commun.*, Vol. 183, No. 1, 86–98, 2012.
17. Shen, J., W. Sha, Z. X. Huang, M. S. Chen, and X. L. Wu, "High-order symplectic FDTD scheme for solving a time-dependent Schrödinger equation," *Comput. Phys. Commun.*, Vol. 184, 480–492, 2013.
18. Gray, S. K. and D. E. Manolopoulos, "Symplectic integrators tailored to the time-dependent Schrödinger equation," *J. Chem. Phys.*, Vol. 104, No. 18, 7099–7112, 1996.
19. Yoshida, H., "Construction of higher-order symplectic integrators," *Phys. Lett. A.*, Vol. 150, No. 5, 262–268, 2008.
20. Sha, W., Z. X. Huang, M. S. Chen, and X. L. Wu, "Survey on symplectic finite-difference time-domain schemes for Maxwell's equations," *IEEE Trans. Antennas Propag.*, Vol. 56, No. 2, 493–500, 2008.